

<sup>1</sup> Sriramula  
Srimatha

<sup>2</sup> Balasubbareddy  
Mallala

<sup>3</sup> Upendar J

## ABC-WOA Optimization Strategy for UPQC Fuzzy PI Tuning



**Abstract:** - Growing numbers of power electronics-based non-linear loads have raised worries about power quality (PQ) problems, which include equipment failures, overheating, and unplanned shutdowns. Power filters have traditionally been used for harmonics elimination, but their limitations in dynamic compensation and size present challenges. The present research presents a new methodology using the Artificial Bee Colony - Whale Optimizations Algorithm (ABC-WOA) to optimize the Unified Power Quality Conditioner (UPQC) controller. Assignment aims to tackle obstacles that come with it. The suggested algorithm's efficacy is clear, as shown from the stabilization of objective function values. Highlighting the expertise of the Proportional-Integral (PI) controller in effectively regulating the DC-link voltage, this study successfully addresses power quality concerns. The analysis of voltage injection emphasizes the significant influence of the controller on the power system, showcasing seamless integration and enhanced power quality. This research provides valuable insights into the application of advanced control algorithms in power systems, specifically in addressing challenges related to non-linear loads and transient conditions.

**Keywords:** Unified Power Quality Conditioner (UPQC), Artificial Bee Colony-Whale Optimization Algorithm (ABC-WOA), PI-controller and Harmonics elimination etc.

### I. INTRODUCTION

Power electronics technology has advanced recently, making it simpler to non-linear loads to be widely used. The non-linear equipment can cause various problems, including unexpected shutdowns, consumer equipment malfunctions, transformer unit overheating, and wiring overheating. The utilization of power converters based on power electronics can lead to a decline in power quality (PQ), leading to increased power losses and subsequent economic losses. The implementation of power filters can help mitigate the issues related to poor quality. Passive filters have traditionally been the preferred solution for addressing harmonics elimination and mitigating power quality (PQ) issues. The limitations of this solution are that it can only accommodate a limited range of harmonic compensation and the equipment is large and cumbersome. However, the output of their system is limited as a result of insufficient dynamic compensation and resonance issues [1], [2].

Active power filters (APF) have been created to efficiently attenuate current and voltage disruptions within power distribution systems in order to overcome these limitations. Reactive power remission, flickering voltage, unbalanced loads, voltage & current harmonics, and other power quality (PQ) problems may all be handled using this technique. Voltage regulation, reactive power remission, load unbalancing remission (while dealing with a three-phase wire), as well as neutral current compensation (four-wire system) are the APF shunt uses. The hybrid Active Power Filter (APF) is utilized to handle and alleviate power quality (PQ) disruptions linked to both voltage and current inside the system[3]. The hybrid APF is commonly recognized as the best option for eliminating voltage and current harmonics simultaneously [4].

Techniques for controlling frequency in the frequency domain include fast Fourier transform, Kalman filtering, and discrete Fourier transform, as well as the heavy computational load placed on digital signal processing (DSP) processors. To deal with these disadvantages, active power filters (APF) have been evolved to successfully reduce power distribution networks' current and voltage disruptions. These approaches have the capability to address a range of power quality (PQ) issues in [5-8]. Harmonic currents, voltage sag/swell, imbalanced three-phase voltage,

<sup>1</sup> \*Sriramula Srimatha: Research Scholar, University college of Engineering, Osmania University, Hyderabad, Telangana, India, Email: srimatha.sri786@gmail.com

<sup>2</sup> Balasubbareddy Mallala: Professor, Chaitanya Bharathi Institute of Technology, Hyderabad, Telangana, India. Email: balasubbareddy79@gmail.com

<sup>3</sup> J. Upendar: Assistant professor, University college of Engineering, Osmania University, Hyderabad, Telangana, India. Email: dr.8500003210@gmail.com

and other power quality issues can all be detected using the harmonic comprehensive detection algorithm, which is based on improved p-q theory in [9]. In recent years, several estimation methods have been utilized, including adaptive notch filter, complex vector filter, as well as phase-locked loop (PLL). Despite, previously discussed parameter estimation controls, the Phase-Locked Loop (PLL) demonstrates effective tracking of supply voltage parameters in [10].

The literature also documents state observer-based control systems in addition to frequency and time domain control mechanisms. Calculating the harmonic component that are existing inside the grid system, the state observer is used [11]. An enhanced method for leveraging the grasshopper optimization algorithm (GOA) to provide strong control over the dynamic voltage restorer and increase power quality in [12]. Second-order generalized integrator-based PLL (SOGI-PLL) is a commonly used PLL due to its straightforward structure, specific filtering capability, and frequency adaptability in [13]. A adaptive full order observer control system, which is based on observer theory and adaptive theory, is to precisely estimate the unknown supply voltage characteristics algorithm is based on adaptive full order observers is described in [14,15]. The operating principle and control strategy based on the dq0 transform are discussed in [16]. The authors are described different algorithms such as (ABC-DE-WOA), (ACWOA), ABC in [17-19]. In [20-27] authors are described different power quality mitigation techniques using conventional and AI based algorithms.

## II. SYSTEM DESCRIPTION

### 2.1 Configuration of the System

A conventional series and shunt conditioner's system setup is shown in Fig. 1. To build combined series and shunt power conditioners (UPQC), the two converters are connected in series and shunt mode using a shared DC connection.

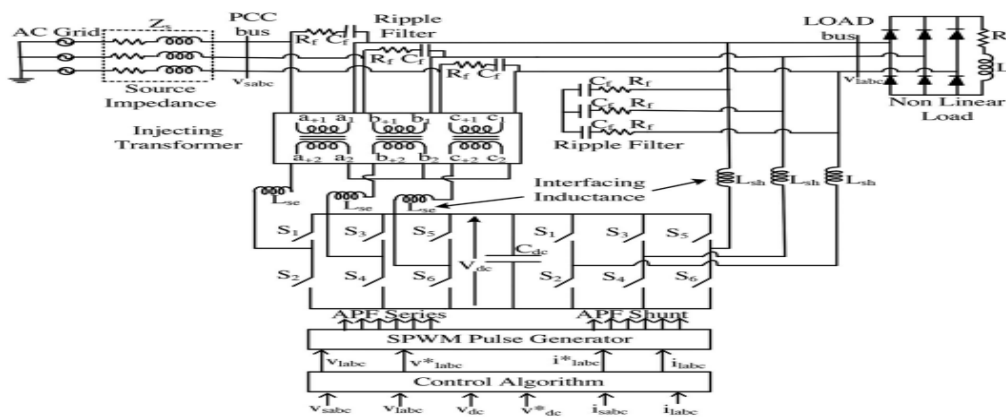
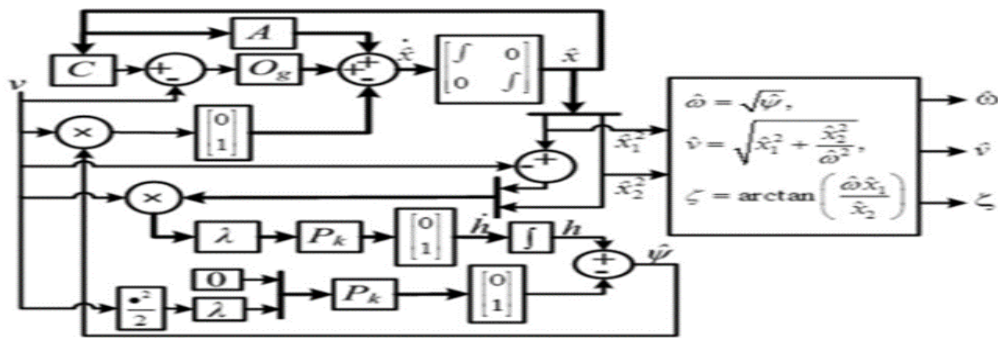


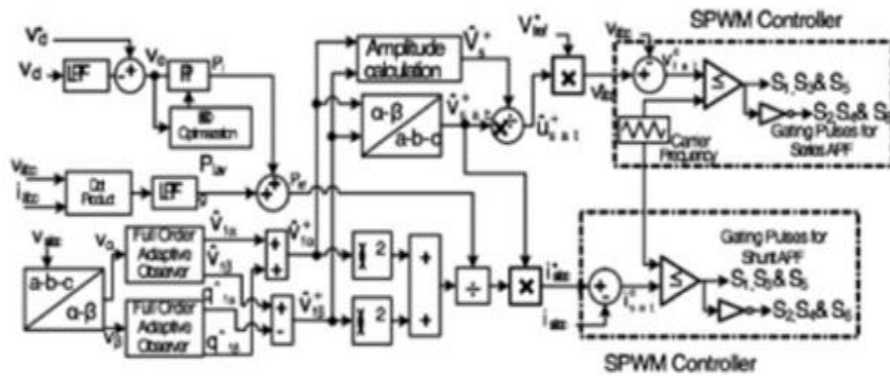
Figure. 1 conventional series and shunt conditioner's system

A direct current capacitor, denoted as  $C_{dc}$ , serves as an energy storage element that is connected in a consecutive arrangement and DC-link voltage is created between the two converters. This DC capacitor's principal function is to set the characteristics of the DC voltage source on the shared DC connection. As a result, it is critical to maintain a power balance between the power going into the direct current connection from the series converter and the power flowing via the shunt converter, and vice versa. The  $L_{se}$  &  $L_{sh}$  converters are interfaced by the use of interfacing inductances. One converter's output is connected to the AC mains in series via a series transformer, while the second converter's output is linked to power distribution network in parallel. Ripple filters, specifically  $R_f$  and  $C_f$ , are utilised to mitigate the harmonics produced as a result of converter switching. Design specifications for Unified Power Quality Conditioner (UPQC), including the characteristics of the suggested control algorithm running under non-linear loads.

2.2 Algorithm for Control



(a) complete order adaptive observer system



(b) voltage reference and generation of current

Figure. 2 Adaptive observer algorithm-based system

The complete order adaptive observer technique block diagram is presents in Fig. 2(a) in [15] & Fig. 2(b) in [15] shows the control scheme Here, the suggested complete order adaptive observer technique is employed to comprehensively illustrate the creation of reference signals for both Active Power Filters (APFs). The switching sequences are obtained through a comparison between the actual utility load voltage and the reference load voltage within the Sinusoidal Pulse Width Modulation (SPWM) controller. The fuzzy (PI) controller's settings may now be adjusted using the ABC-WOA algorithm methodology, which takes the place of the conventional manual tuning method. Organised per sub-part, this section provides a thorough explanation of each of the control algorithm's components.

2.3 Using a complete order adaptive observer for parameter estimates and design

The voltage supply is denoted by  $asv = V_p \sin(\omega t + \theta) = V_p \sin \zeta$ . Where  $V_p$  represents the grid voltage amplitude,  $\omega$  is the angular frequency of grid, as well as phase angle  $\zeta = [0, 2\pi]$ . The supplied grid voltage as well as its derivative model are represented by the following formulae.

$$\dot{x} = \bar{A}x \tag{1}$$

Where  $x = \begin{bmatrix} x_1 \\ x_2 \end{bmatrix} = \begin{bmatrix} v \\ \dot{v} \end{bmatrix} = \begin{bmatrix} V_p \sin(\omega t + \theta) \\ V_p \omega \cos(\omega t + \theta) \end{bmatrix}; \bar{A} = \begin{bmatrix} 0 & 1 \\ -\psi & 0 \end{bmatrix}$  with  $\psi = \omega^2$ .

Therefore,  $\dot{x} = \begin{bmatrix} 0 & 1 \\ -\psi & 0 \end{bmatrix} \begin{bmatrix} V_p \sin(\omega t + \theta) \\ V_p \omega \cos(\omega t + \theta) \end{bmatrix} = \begin{bmatrix} V_p \sin(\omega t + \theta) \\ -\omega^2 V_p \cos(\omega t + \theta) \end{bmatrix}$  (2)

The instrument's output y components must be connected to the input grid voltage because the parameter 'x' have a relationship with both grid voltage as well as it's derivative.

$$y = Cx \tag{3}$$

The C value is represented by the matrix [1 0]. Based on equations (1) and (3), it can be concluded that the system's rank  $[CC\bar{A}]^T = 2$  is observable, with  $\omega$  representing the system frequency. The parameter associated with grid voltage in the dynamic system model (1). In the subsequent section, a proposed adaptive observer is presented for system (1) with the objective of achieving zero steady state error. The observer purpose is to estimate both the state variable  $x$  as well as the fundamental frequency  $\omega$ . The matrix A, denoted as  $A = \begin{bmatrix} 1 & 0 \\ 0 & 0 \end{bmatrix}$ , is adjusted for the purpose of an observable dynamic system in order to derive the complete order adaptive observer.

$$\dot{\hat{x}} = Ax - \begin{bmatrix} 0 \\ \hat{\psi} \end{bmatrix} y + O_g (C\hat{x} - y), \quad x(0) = x_0 \tag{4}$$

$A_k = A + O_g C$  is Hurwitz, the provided system (4) is likewise observable and possesses observer gain matrix  $O_g$ . This contributes to the existence of,  $P_k = P_k^T > 0$  and  $Q_k = Q_k^T > 0$

$$A_k^T P_k + P_k A_k = -Q_k < 0 \tag{5}$$

As a result, estimate errors  $\tilde{x} = \hat{x} - x$  and  $\tilde{\psi} = \hat{\psi} - \psi$  may be specified for state  $x$  as well as unknown parameter to filter out throughout the procedure. By using (5) to replace the dynamic estimated error in system (4),

$$\dot{\hat{x}} = A_k \tilde{x} - \begin{bmatrix} 0 \\ \tilde{\psi} \end{bmatrix} y \tag{6}$$

To produce a dynamic system with error correction, the Lyapunov function must be built.  $P_k$  is chosen as the positive semi-definite matrix for designing Lyapunov function.

$$V(\tilde{x}, \tilde{\psi}) = \tilde{x}^T P_k \tilde{x} + \frac{1}{\lambda} \tilde{\psi}^2 \tag{7}$$

when the parameter is greater than 0. As a result, the derivative  $V(\tilde{x}, \tilde{\psi})$  can written as,

$$\dot{V}(\tilde{x}, \tilde{\psi}) = -\tilde{x}^T Q_k \tilde{x} - \tilde{x}^T P_k \begin{bmatrix} 0 \\ 1 \end{bmatrix} y \tilde{\psi} + \frac{2}{\lambda} \tilde{\psi} \dot{\tilde{\psi}} \tag{8}$$

Since  $\psi$  is always the same, we can lower it, and the possible adaptive update rule can be written as,  $\dot{\tilde{\psi}} = \tilde{\psi}$

The following states may be created from system (1),  $x_1 = y$  and  $x_2 = \dot{x}_1 = \dot{y}$ , which changed the (8) as the following equation.

$$\dot{\tilde{\psi}} = \lambda [\hat{x}_1 - y \hat{x}_2] P_k \begin{bmatrix} 0 \\ 1 \end{bmatrix} y - \lambda \begin{bmatrix} 0 & y \end{bmatrix} P_k \begin{bmatrix} 0 \\ 1 \end{bmatrix} y \tag{9}$$

$$\hat{\psi}(0) = \hat{\psi}_0$$

The dynamics of the state variable  $b$  are modified by an adaptive observer as

$$\dot{b} = \lambda [\hat{x}_1 - y \hat{x}_2] P_k \begin{bmatrix} 0 \\ 1 \end{bmatrix} y, b(0) = b_0 \tag{10}$$

By inserting (8) into equation (11) and integrating on both sides of equation (10), the following expression is obtained:

$$\begin{aligned} \hat{\psi} = b - \lambda \begin{bmatrix} 0 & \frac{y^2}{2} \end{bmatrix} P_k \begin{bmatrix} 0 \\ 1 \end{bmatrix} y + \hat{\psi}(0) \\ - b(0) + \lambda \begin{bmatrix} 0 & \frac{y(0)^2}{2} \end{bmatrix} P_k \begin{bmatrix} 0 \\ 1 \end{bmatrix} \end{aligned} \tag{11}$$

$$\hat{\psi} = b - \lambda \begin{bmatrix} 0 & \frac{y^2}{2} \end{bmatrix} P_k \begin{bmatrix} 0 \\ 1 \end{bmatrix} \tag{12}$$

We may use the derivatives of the Lyapunov function (8) to verify whether the observer is stable and if the projected states are true at steady state by substituting (10) and (12),

$$\dot{V}(\tilde{x}, \tilde{\psi}) = -\tilde{x}^T Q_k \tilde{x} \leq 0 \quad \dot{V}(\tilde{x}, \tilde{\psi}) = -\tilde{x}^T Q_k \tilde{x} \leq 0 \tag{13}$$

The closed loop system, which has been formed using components (4), (10), and (12), can be concluded to be globally stable. The filtering term, which is obtained using the observer gain matrix  $O_g(C\hat{x} - y)$ , does not have any impact on the system model once the steady state is achieved, where  $\hat{x}$  equals  $x$ . In cases where  $\hat{x} \neq x$ , the stability of the dynamic error can be ensured if the AC matrix is Hurwitz.

$$\hat{\omega} = \sqrt{\tilde{\psi}}, \quad \tilde{v} = \sqrt{\hat{x}_1^2 + \frac{x_2^2}{\hat{\omega}^2}} \quad \text{and} \quad \zeta = \arctan\left(\frac{\hat{\omega}\hat{x}_1}{\hat{x}_2}\right) \tag{14}$$

### III. METHOD

#### 3.1 Self-Learning Fuzzy Controllers Based on ABC-WOA

#### 3.2 Fuzzy Logic Control System

An enclosed-loop fuzzy control system is shown in the Fig. 3. To account for non-fuzzy variables with definite values, both the command and plant output are subjected to fuzzification. Moreover, the controlled plant's inability to respond directly to fuzzy logic controls necessitates the defuzzification of the fuzzy logic control generated by the fuzzy algorithm before applying it to the plant. The rule basis consists of uncertain rules, while the database includes membership functions for corresponding fuzzy subsets. Fuzzy rules include potential elements such as fuzzy variables, fuzzy subsets identified by membership functions, and a conditional statement.

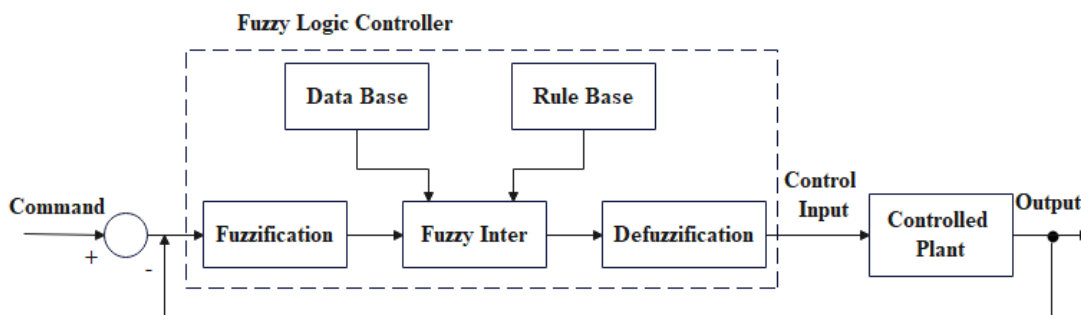


Figure.3 Enclosed-loop fuzzy control system

#### 3.3 Fuzzy PI Control Based Rules

Consider a fuzzy PI controller under consideration to have two inputs and one output. The error signal  $e$  and change-of-error are two input fuzzy variables of the FLC; the incremental input is the output fuzzy variable of the FLC. It is possible to combine the set of unclear rules in issue into a single rule by applying the union operator that is explained in Eq.16.

$$R = R_1 \cup R_2 \cup \dots \cup R_l \tag{16}$$

After applying the max-min inference technique, we obtain a fuzzy output value. To convert this into a precise value, we need to perform the de-fuzzification process. The center-of-gravity method is commonly used for this purpose. In this approach, we calculate the weighted average of the final fuzzy output's membership function curve to determine the most representative crisp value. The centroid de-fuzzification technique is useful in applications where a well-defined value is required.

$$\Delta u = (e \text{ and } e_c) \circ R \tag{17}$$

$$\mu_c(\Delta u) = \max_{e, e_c} \left\{ \min \left( \mu_{A_i}(e), \mu_{B_i}(e_c), \mu_R(e, e_c, \Delta u) \right) \right\} \tag{18}$$

The resulting output  $\Delta u$  can be shown as

$$\Delta u^* = \frac{\sum_{i=1}^l \Delta u_i \mu_c[\Delta u_i]}{\sum_{i=1}^l \mu_c[\Delta u_i]} \tag{19}$$

### 3.4 Fuzzy Control Decision table

The weighted absolute error and the weighted absolute error change added together provide the performance index, which is defined as the reciprocal of this sum:

Table. 1 Fuzzy Control Decision Table

		$e \uparrow$							
		NB	NM	NS	Z	PS	PM	PB	
$\Delta u \swarrow$	PB	Z	PS	PM	PB	PB	PB	PB	
	PM	NS	Z	PS	PM	PB	PB	PB	
	PS	NM	NS	Z	PS	PM	PB	PB	
	Z	NB	NM	NS	Z	PS	PM	PB	$e_c \rightarrow$
	NS	NB	NB	NM	NS	Z	PS	PM	
	NM	NB	NB	NB	NM	NS	Z	PS	
	NB	NB	NB	NB	NB	NM	NS	Z	

### 3.5 Fitness Function

The fitness function of a fuzz proportional-integral (PI) controller refers to the measurement of its performance using a specific set of criteria. This is the situation in which the advantages of the controller are being optimized. The objective is to create a function of fitness that accurately represents the intended behavior of the system's controls & can be utilized through optimization methods to assess and enhance the controller gains.

$$F = \frac{1}{\sum_{j=1}^k (w_1 |e(j)| + w_2 |e_c(j)|)} \tag{20}$$

### 3.6 Artificial Bee Colony (ABC) Optimization algorithm

In ABC is mechanical bee colony, there are three distinct species: scout bees, who look for food sources at random, server bees, which are entrusted with locating particular food sources, and worker bees, who watch the utilised bees dancing about the hive in quest of food. Because of their unemployment, observers and observers are frequently referred to as jobless beekeepers. The initial job for the scout bees is to locate every food source.

### 3.7 Initialization Phase-

The population of food source vectors (m=1....SN, SN:) is started by the scout bees, who also establish the control settings. When establishing the framework, one might apply the following definition.

$$y_{mx} = l_x + \text{rand}(0,1) * (u_x - l_x) \tag{21}$$

3.8 *Employees Bees Phase-*

Makes use of Bees would seek out new nectar-rich food sources that are near to ones they have visited and remembered. They scour the area for possible food sources and assess their suitability (viability).

$$v_{mx} = y_{mx} + f_{mx} (y_{mx} - y_{kx}) \tag{22}$$

3.9 *Onlooker Bees phase-*

Bees that are unemployed may be divided into two groups: scout bees and spectator bees. One may use the term given in the equation to calculate the probability that an observer bee would choose.

$$p_m = \frac{\text{fit}_m(\tilde{y}_m)}{\sum_{m=1}^{SN} \text{fit}_m(\tilde{y}_m)} \text{ where } \text{fit}_m \text{ is fitness function} \tag{23}$$

3.10 *Hybrid Optimization Model*

This study utilized a hybrid ABC-WOA optimization method to specifically select relevant features associated with soil moisture and temperature data from the provided dataset. This feature selection process aimed to enhance the accuracy and efficacy of our study's predictive models in the context of smart irrigation systems.

---

**Algorithm: Hybrid ABC-WOA Optimization**

---

Initialization: Initialize ABC and WOA populations randomly:

- ABC population: N\_ABC bees
- WOA population: N\_WOA whales

Repeat for a maximum of max\_iterations or until termination criteria are met:

For each ABC bee in ABC population:

- Employed bees explore solutions locally:
  - Modify the position of bee using a local search strategy.
  - Calculate the fitness of each employed bee.
- Onlooker bees select employed bees based on fitness and perform global search:
  - Select employed bees probabilistically.
  - Apply global search strategy.

Evaluate fitness of onlooker bee.

For each WOA whale in WOA population:

- Update whale position using WOA equations:
 
$$X_{WOA\_j} = A * \sin(B) * |C * X_{rand} - X_{WOA\_j}| - X_{WOA\_j}$$
- Evaluate fitness of WOA whale.

---

3.11 *Fuzzy PI Control Algorithm with ABC-WOA Basis for Self-Learning*

A comprehensive procedure for implementing a self-learning fuzzy PI control algorithm using the ABC-WOA (Artificial Bee Colony - Whale Optimisation Algorithm) approach. And the integration of ABC and WOA presents a hybrid optimisation approach for the fine-tuning of the fuzzy PI controller.

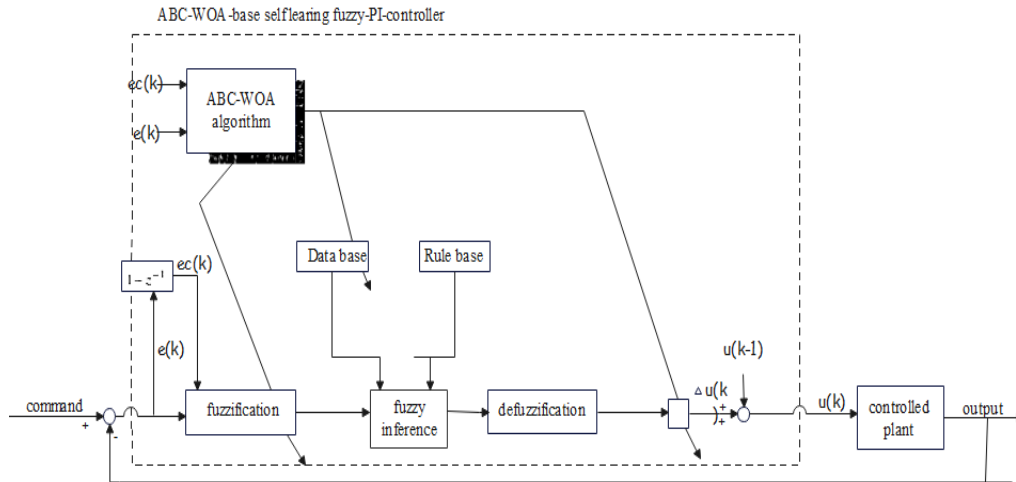


Figure. 4 self-learning fuzzy PI control algorithm using the ABC-WOA.

- Step-1: Create the fuzzy control decision table after figuring out how many fuzzy subgroups there are for each fuzzy variable ( $e, e_c, \Delta u$ ).
- Step-2: Describe the fitness function based on the control system's performance criteria, as mentioned in eq. (22) or adapt it to accommodate the hybrid nature of ABC and WOA.
- Step-3: Calculate the number of people, crossover percentage, change rate, generation number, and any other parameters unique to the ABC-WOA algorithm.
- Step-4: Define the parameters ( $a, b, g, f_{norm}$ ) bit string range and length, then generate a random starting generation of chromosomes.
- Step-5: Regarding every chromosome within the population: 1. Determine the error ( $e$ ) & error change ( $e_c$ ). 2. Put this fuzzy PI control law, fuzzy inference, de-fuzzification, and fuzzification phases into practice. 3. Assess each population's fitness ratings for this generation.
- Step 6: Reproduce New Generation (ABC)
- Step 7: Apply the WOA algorithm to enhance exploration and exploitation, and utilize WOA's search mechanism to explore the solution space and refine solutions.
- Step8: Apply crossover and mutation operations based on the rates determined in Step 3, using the WOA algorithm.
- Step 9: Arrange the population in previous generation with the highest fitness value for the future generation (elitism).
- Step 10: Iteratively replicate Steps 5 through 9 until the specified number of generations is reached.
- Step 11: Determine associated parameter values ( $a, b, g,$  and  $f_{norm}$ ) for the chromosome that has the highest fitness value throughout all generations.
- Step 12: Stop the Algorithm.

The optimal fuzzy (PI) controller gains are computed using the optimum cost function  $F(K)$  of 1935 via execution of the technique in the MATLAB/SIMULINK environment, as illustrated in Fig. 5. When these values are used, U When compared to trails and error techniques values, UPQC offers a better response. This enhances the UPQC controller's ability to raise power quality.

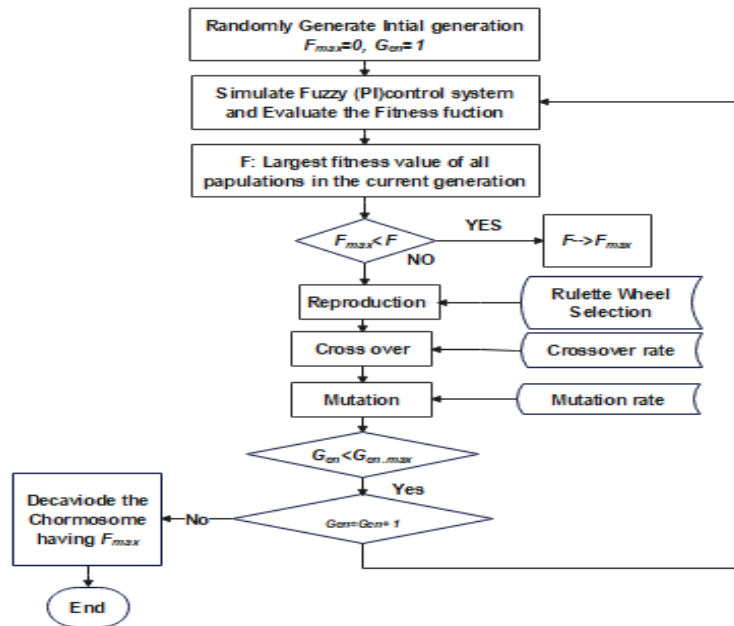


Figure. 5 Flow diagram for the suggested fuzzy PI control algorithm based on ABC-WOA

In Fig. 6, the DC-link voltage is displayed in its enlarged form together with the previously described PQ issues. This allows you to assess the effectiveness as well as PI controller responsiveness using the BBO method. A magnified view of the changes in the maximum peak overshoot (Mp), settling time (ts), and rising time (tr) for both tuning techniques is shown in Fig. 7. A 100% final value rise time, or 700, and a tolerance band of 2%, or 686-714, are ideal for an underdamped system.

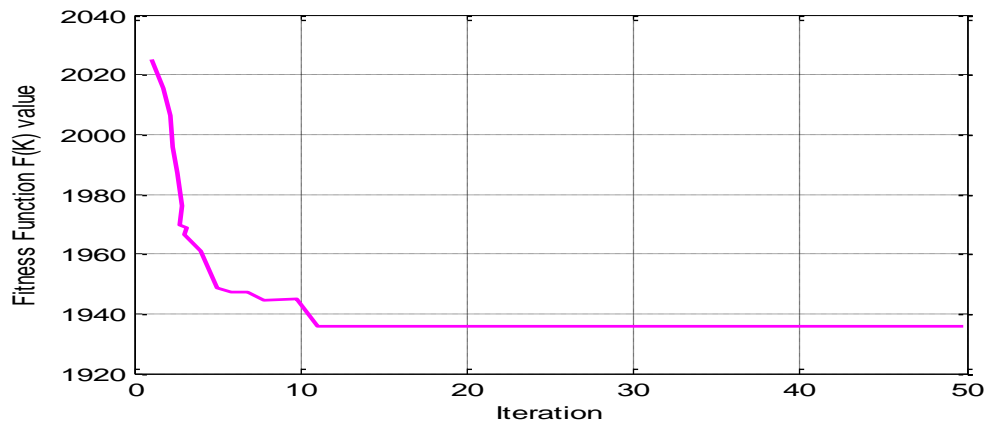


Figure.6 Iteration-specific objective function

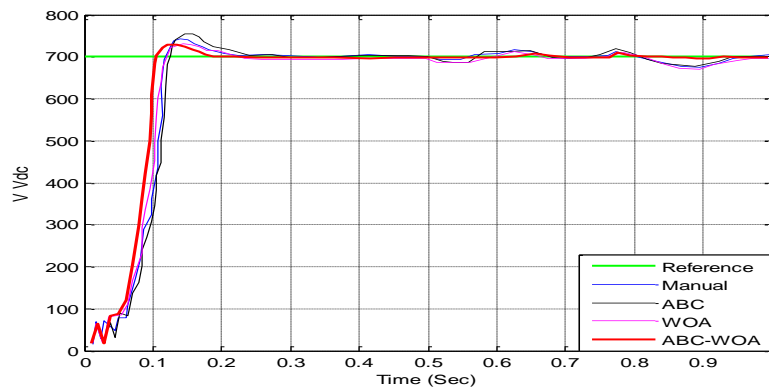


Figure. 7 Performance of ABC-WOA in tuning

## IV. RESULTS AND DISCUSSION

## 4.1 Sub section PV-ARRAY parameters

Equations should be placed at the center of the line and provided consecutively with equation numbers in parentheses flushed to the right margin, as in (1). The use of Microsoft Equation Editor or Math Type is preferred.

Table. 2 PV-ARRAY Parameters

Elements	Values
Max Power (W)	234.986
Cells per module (Ncell)	60
Open circuit voltage Voc (V)	37
Short-circuit current Isc (A)	8.54
Voltage at max power point Vmp (V)	29.34
Current at max power point Imp (A)	8.02
Temp coefficient of Voc (%/deg.C)	-0.369
Temp coefficient of Isc (%/deg.C)	0.087

The simulation was performed utilizing Matlab 2021a on a computing system featuring an i5core processor, 8GB of RAM, and a 256GB hard disk. In particular, this setup proves instrumental in evaluating the performance of the ABC-WOA tuned UPQC controller under dynamic load conditions.

## 4.2 System Parameters

The system parameters for the photovoltaic (PV) array are in outlined as follows in Table. 3. These parameters collectively define the electrical characteristics and performance attributes of the PV array.

Table. 3 Three phase Series RLC

Elements	Values
Resistance R (Ohms):	0.4
Inductance L (H):	15e-3
Resistance (Ohms): RL	30

The three-phase series RLC (Resistance-Inductance-Capacitance) elements for the system are specified with the following values in Table.3. These elements collectively define the impedance characteristics of the three-phase circuit, where the resistance represents the dissipative component, the inductance accounts for the energy storage in the magnetic field, and the second resistance (RL) potentially signifies additional resistive effects in the circuit.

Table. 4 Controllers

Controllers	THD Values
PI	0.87 ± 0.3
Fuzzy PI	0.9 ± 1
Fuzzy ABC-WOA	0.97 ± 0.1

Among the considered controllers, namely Proportional-Integral (PI), Fuzzy PI, and Fuzzy ABC-WOA, the Fuzzy ABC-WOA controller stands out as the most effective based on the provided values in Table. 4. The Fuzzy ABC-WOA controller's superior performance, indicated by the highest mean value and the narrowest range of uncertainty, suggests its efficacy in tuning and optimizing the system. Therefore, in light of these results, the Fuzzy ABC-WOA controller emerges as the preferred choice among the evaluated controllers, showcasing its potential for enhanced control and optimization in the given context.

The primary aim of simulation model's main goal is to assess the effectiveness UPQC (Unified Power Quality Conditioner) controller constructed using the ABC-WOA (Artificial Bee Colony - Whale Optimisation Algorithm) under dynamic load circumstances. The load of the system experiences changes between the duration of 0.5 to 0.7

seconds, indicating a transient phase where the controller's reaction to different electrical loads is monitored. The application of the ABC-WOA algorithm for the purpose of tuning the UPQC controller proposes an optimisation procedure aimed at improving its efficacy.

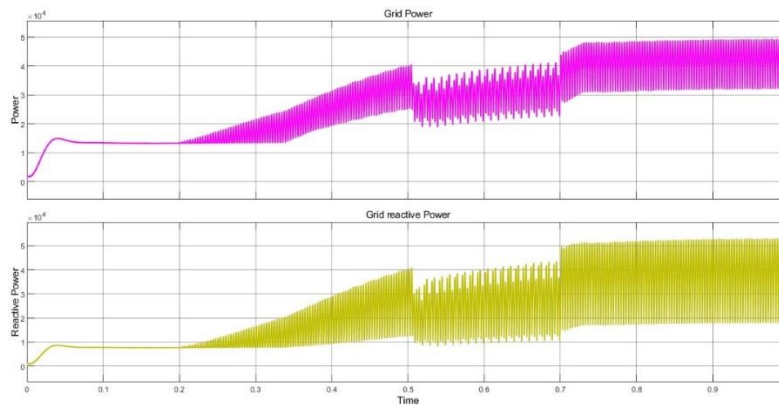


Figure. 8 Grid Real and Reactive Power

The Fig. 8 illustrates the variations in grid active & reactive power. It's observed that the grid active power experiences significant fluctuations within the range of 0.5 to 0.7. The grid's reactive power exhibits relatively moderate fluctuations, ranging between 0.5 and 0.7. The reactive power of the grid demonstrates significant fluctuations over time, characterized by multiple distinct peaks and dips observed within the depicted timeframe. Both lines exhibit a gradual upward trend over the course of time.

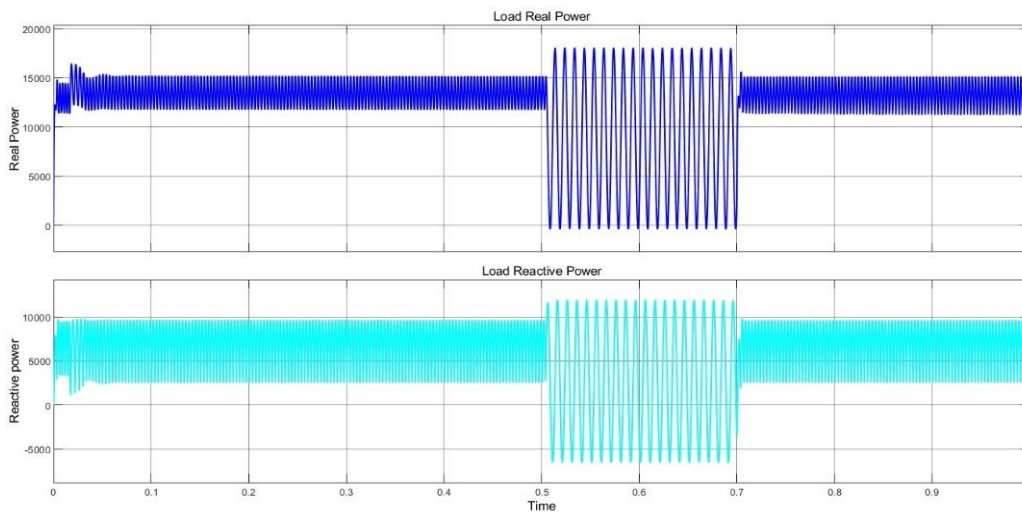


Figure. 9 Load Real and Reactive Power

The Fig. 9 observation indicates the temporal variations in both real & reactive power load consumptions. The abrupt reduction in both real & reactive power observed at the 30-second mark indicates the occurrence of a load change event during that period. The power graph exhibits a consistent value of approximately 15,000 kW during the initial 30-second period, followed by a significant decline to approximately 5,000 kW. The graph depicting reactive power illustrates an initial value of approximately 3,000 kilovolt-ampere reactive (kVAR) for the initial 30-second period, subsequently exhibiting a significant decline to approximately 1,000 kVA.

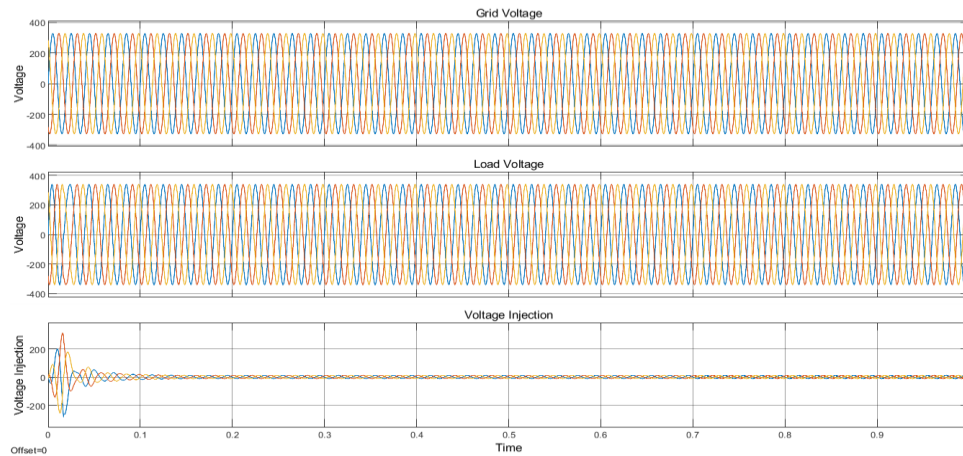


Figure. 10 Voltage Injection

The Fig. 10 illustrates four voltage graphs plotted against time. The first graph illustrates the grid voltage, denoting the voltage provided by the utility company. The second graph illustrates a load voltage, which represents voltage at specific location where power is consumed by customer. The third graph illustrates voltage injection, which refers to the application of a voltage signal into the system with the purpose of enhancing its performance. The grid voltage remains consistently at 400V AC, characterized by a sinusoidal waveform. The load voltage exhibits a sinusoidal waveform, albeit with reduced amplitude compared to the grid voltage, and possesses a higher frequency. The voltage injection comprises a triangular waveform that is overlaid onto the load voltage. The resultant voltage is a sinusoidal waveform that exhibits slight distortion due to the presence of the triangular waveform.

## V. CONCLUSION

In conclusion, this study thoroughly assesses the Unified Power Quality Conditioner (UPQC) controller performance which has been tuned using the Artificial Bee Colony - Whale Optimization Algorithm (ABC-WOA) in the presence of dynamic load conditions. The algorithm's effectiveness was demonstrated through simulations conducted on a robust computing system. The objective function values were stabilized after the 11th iteration. The amplified perspective showcases the PI controller proficiency in effectively regulating the DC-link voltage, thereby effectively addressing concerns related to power quality. The dynamic system nature is highlighted by the comprehensive examination of grid and load voltages, real and reactive powers, and power factor. Notably, significant load changes occur at the 30-second mark. The results of this study confirm that the ABC-WOA-tuned UPQC controller is effective in addressing transient phases and load variations. The analysis of voltage injection highlights the significant influence of the controller on the power system. It demonstrates the successful integration of the controller, resulting in improved power quality. These findings have the potential to facilitate real-world applications involving non-linear loads and transient conditions.

## REFERENCES

- [1] S. Poongothai and S. Srinath, "Power quality enhancement in solar power with grid connected system using UPQC," *Microprocess. Microsyst.*, vol. 79, no. October, p. 103300, 2020, doi: 10.1016/j.micpro.2020.103300.
- [2] S. K. Dash and P. K. Ray, "A New PV-Open-UPQC Configuration for Voltage Sensitive Loads Utilizing Novel Adaptive Controllers," *IEEE Trans. Ind. Informatics*, vol. 17, no. 1, pp. 421–429, 2021, doi: 10.1109/TII.2020.2986308.
- [3] S. C. Devi, B. Singh, and S. Devassy, "Modified generalised integrator based control strategy for solar PV fed UPQC enabling power quality improvement," *IET Gener. Transm. Distrib.*, vol. 14, no. 16, pp. 3127–3138, 2020, doi: 10.1049/iet-gtd.2019.1939.
- [4] F. Nkado, F. Nkado, I. Oladeji, and R. Zamora, "Optimal Design and Performance Analysis of Solar PV Integrated UPQC for Distribution Network," *Eur. J. Electr. Eng. Comput. Sci.*, vol. 5, no. 5, pp. 39–46, 2021, doi: 10.24018/ejece.2021.5.5.361.
- [5] K. Srilakshmi, C. N. Sujatha, P. K. Balachandran, L. Mihet-Popa, and N. U. Kumar, "Optimal Design of an Artificial Intelligence Controller for Solar-Battery Integrated UPQC in Three Phase Distribution Networks," *Sustain.*, vol. 14, no. 21, 2022, doi: 10.3390/su142113992.

- [6] Amirullah, A. Soeprijanto, Adiananda, and O. Penangsang, "Power Transfer Analysis Using UPQC-PV System under Sag and Interruption with Variable Irradiance," *Proceeding - ICoSTA 2020 2020 Int. Conf. Smart Technol. Appl. Empower. Ind. IoT by Implement. Green Technol. Sustain. Dev.*, 2020, doi: 10.1109/ICoSTA48221.2020.1570615953.
- [7] Kwan, K.H., et al.: Unified power quality conditioner for improving power quality using MVR with Kalman filters. In *Proceedings of the International Power Engineering Conference*, vol. 2, pp. 980–985. Singapore 2005.
- [8] J. C. Das, "Passive filters - potentialities and limitations," in *IEEE Transactions on Industry Applications*, vol. 40, no. 1, pp. 232-241, Jan.-Feb. 2004, doi: 10.1109/TIA.2003.821666.
- [9] Shen, S., et al.: UPQC Harmonic detection algorithm based on improved p-q theory and design of low-pass filter. In *Proceedings of the Chinese Control and Decision Conference (CCDC)*, pp. 5156–5160. Shenyang, China, 9–11 June 2018.
- [10] Emadi, A.N., Bekiarov, S.B.: *Uninterruptible Power Supplies and Active Filters*, CRC Press, Boca Raton, FL (2005).
- [11] Kumar, N.G., et al.: A novel orthogonal current decomposition control for grid-connected voltage source converter. *IEEE Trans. Ind. Appl.* 55(6), 7628–7641 (2019).
- [12] Omar, I., et al.: "An improved approach for robust control of dynamic volt-age restorer and power quality enhancement using grasshopper optimization algorithm". *ISA Trans.* 95, 110-129 (2019).
- [13] J. Xu, H., et al.: "Overview of SOGI-Based Single-Phase Phase-Locked Loops for Grid Synchronization Under Complex Grid Conditions," in *IEEE Access*, vol. 9, pp. 39275-39291, 2021, doi: 10.1109/ACCESS.2021.3063774.
- [14] Sayed Javed Alam, Sabha Raj Arya, "Observer-based control for UPQC-S with optimized gains of PI controller", April 2020 *International Transactions on Electrical Energy Systems* 30(2):e47233 DOI:10.1002/2050-7038.12406.
- [15] Sayed Javed Alam, et al.: "Biogeography based optimization strategy for UPQC PI tuning on full order adaptive observer-based control", November 2020, *IET Generation, Transmission & Distribution* 15(5) DOI:10.1049/gtd2.12020.
- [16] Long, Y., et al.: MMC-UPQC: Application of modular multilevel converter on unified power quality conditioner. In *Proceedings of the IEEE Power & Energy Society General Meeting*, pp. 1–5. Vancouver, BC, Canada, 21–25 July 2013.
- [17] T. Siahmarzkooh and M. Alimardani, "A Novel Anomaly-based Intrusion Detection System using Whale Optimization Algorithm WOA-Based Intrusion Detection System," ... *J. Web Res.*, no. December 2021.
- [18] P. K. D, S. BJ, A. Kanavalli and A. Vincent, "ABC-DE-WOA: A New Hybrid Algorithm for Optimization Problems," 2022 4th International Conference on Circuits, Control, Communication and Computing (I4C), Bangalore, India, 2022, pp. 501-506, doi: 10.1109/I4C57141.2022.10057946.
- [19] NM Spencer Prathap Singh and N Kesavan Nair, "Artificial bee colony algorithm for inverter complex wave reduction under line-load variations", *Transactions of the Institute of Measurement and Control*, 2017, DOI: 10.1177/0142331216687019
- [20] Srimatha, S., Mallala, B. & Upendar, J., A Novel ANFIS-controlled customized UPQC device for power quality enhancement. *Journal of Electrical Systems and Inf Technol* 10, 55 (2023). <https://doi.org/10.1186/s43067-023-00121-1>.
- [21] M Balasubbareddy, P Venkata Prasad, Saini Varshini (2021), "A Novel Power Quality Conditioner with UPQC", *GIS Science journal*, Vol.8, Issue 3, pp. 1171-1179, March 2021 DOI:20.18001.GSJ.2021.V8I3.21.36786.
- [22] Saini Varshini and M Balasubbareddy, "Power Quality Improvement using Fuzzy Logic Controller Based UPQC", *PROTEUS JOURNAL*, Vol.12, Issue 6 pp.1-9, June 2021 <https://doi.org/10.37896/PJ12.06/0351>.
- [23] Balasubbareddy Mallala, Venkata Prasad Papan, Kowstubha Palle, Power Quality Conditioner with Hybrid Ant Colony Optimization, *International Conference on Evolutionary Artificial Intelligence (ICEAI 2023)*, at RVS College of Engineering & Technology, Coimbatore, India, 13-14, September 2023.
- [24] Balasubbareddy, M., Venkata Prasad, P., Palle, K. Power Quality Conditioner with Fuzzy Logic Controller. In: Kaiser, M.S., Xie, J., Rathore, V.S. (eds) *Information and Communication Technology for Competitive Strategies (ICTCS 2022)*. Lecture Notes in Networks and Systems, vol 615. Springer, Singapore. [https://doi.org/10.1007/978-981-19-9304-6\\_56](https://doi.org/10.1007/978-981-19-9304-6_56)
- [25] Mallala, B., Prasad, P.V., Palle, K. Analysis of Power Quality Issues and Mitigation Techniques Using HACO Algorithm. In: Raj, J.S., Perikos, I., Balas, V.E. (eds) *Intelligent Sustainable Systems. ICoISS 2023*. Lecture Notes in Networks and Systems, vol 665. Springer, Singapore. [https://doi.org/10.1007/978-981-99-1726-6\\_65](https://doi.org/10.1007/978-981-99-1726-6_65)
- [26] Balasubbareddy, M., Sri Ram, K.V., Sangu, R. Modeling and Design of FPGA-Based Power Quality Analyzer. In: Biswas, A., Islam, A., Chaujar, R., Jaksic, O. (eds) *Microelectronics, Circuits and Systems. Lecture Notes in Electrical Engineering*, vol 976. Springer, Singapore. [https://doi.org/10.1007/978-981-99-0412-9\\_39](https://doi.org/10.1007/978-981-99-0412-9_39)
- [27] Balasubbareddy, M., Sangu, R. Design of Hardware Unified Power Quality Conditioner to Mitigate Sag and Swell. In: Biswas, A., Islam, A., Chaujar, R., Jaksic, O. (eds) *Microelectronics, Circuits and Systems. Lecture Notes in Electrical Engineering*, vol 976. Springer, Singapore. [https://doi.org/10.1007/978-981-99-0412-9\\_40](https://doi.org/10.1007/978-981-99-0412-9_40).